



Finite Element Method for Simulation of Frozen Potato Tempering in Microwave and Microwave Infrared Oven

Nalan Yazicioglu¹



Received: 13 July 2022 / Accepted: 1 December 2022 / Published online: 28 December 2022
© The Author(s), under exclusive licence to European Association for Potato Research 2022

Abstract

Heat transfer equations solved by the finite element method can be used to understand how foods' temperature changes during tempering. In this paper, the transient temperature change of frozen potato puree tempered in microwave and microwave infrared combination oven was simulated by the finite element method, separately. Maxwell equations were used to calculate the microwave power. Thermal and dielectric properties varied with temperature. Experimental temperature data obtained from the data of the same oven in a previous study for different positions of potato puree were used to validate the simulations developed for different microwave (30, 40, and 50%) and microwave (30, 40, and 50%)-infrared power (10%) combinations. The alteration of temperature according to position in the frozen mashed potato sample was simulated. Port input power for microwave heating by time was obtained. Average root mean square error (RMSE) between literature experimental temperature data and the simulation model was in good agreement with 0.76 °C for microwave and 0.90 °C for microwave and infrared combinations. Microwave and infrared powers' effects on the rate of heat transfer of potato puree were also studied.

Keywords Infrared · Maxwell Law · Microwave · Modeling

Introduction

Microwave heating of food has gained popularity since it has advantages such as increasing the nutritional quality of products and improving food processing effectiveness. Food is heated internally by microwave energy which leads to a faster heating process and a short processing time (Ramaswamy and Tang 2008). These advantages make microwave heating a preferred processing method for defrosting, mainly thawing and tempering. Thawing is the complete process when no ice is present in the food and the food has reached 0 °C at the thermal center.

✉ Nalan Yazicioglu
nalan.yazicioglu@sbu.edu.tr

¹ Gulhane Health Science Faculty, University of Health Sciences, 06018 Ankara, Turkey

Tempering occurs as the temperature at the thermal center of the food reaches -5 to -2 °C, just below the freezing point (James et al. 2017).

The variation of dielectric properties with temperature is critical in thawing and tempering processes. Because one of the most important factors affecting the variation of dielectric constant and dielectric loss factor with temperature was the free and bound water content of foods (Calay et al. 1994), it was shown that both dielectric constant and dielectric loss factor are affected by the change of temperature during the tempering of three frozen dishes. These dielectric properties were found to change slightly at thawed temperature range (Klinbun and Rattanadecho 2017).

In the electromagnetic spectrum, infrared is present between ultraviolet and microwave, as invisible radiant energy (Sepúlveda and Barbosa-Cánovas 2003). In contrast with microwave energy, because of the shorter wavelength, infrared energy does not penetrate into foods deeply. When infrared heating is applied to food, the surface temperature increases and the heat is transferred into the food by conduction (Erdogdu et al. 2018). A limited number of studies are available for numerical modeling of the infrared thawing process (Taher and Farid 2001; Basak 2003; Seyhun et al. 2009).

The rapid change in dielectric properties brings the problem of uneven heating, run-away heating, and surface sogginess. To overcome these problems, modeling using mathematical relations and using infrared heating would be profitable to understand and limit uneven heated spots. Surface sogginess can be decreased by infrared thawing since infrared thawing applies radiation to provide heat which leads to high rate of surface heat transfer and surface removal of water (Venugopal 2005).

Modeling microwave and microwave infrared combination heating is a complicated and important task. The heat generation during microwave heating can be calculated by solving Maxwell's equations, where a heat source term is obtained from the electric field (Rattanadecho et al. 2002; Dincov et al. 2004; Vegh and Turner 2006). The second approach is to estimate the heat generation by Lambert's Law that depends on the penetration depth of the microwave inside the product (Seyhun et al. 2009; Pitchai et al. 2015; Singh et al. 2020). Whilst there is no need to calculate the electromagnetic field inside the heated food with the Lambert approach, the electromagnetic field is calculated for the Maxwell equation approach (Curet et al. 2008).

Campañone and Zaritzky (2010) used Lambert's Law, obtaining the numerical solution using an implicit Crank-Nicolson finite difference method to predict the temperature profile during thawing of frozen meat and validated their approach using experimental data from previously published studies. Since food has complex compositions, model foods were obtained and found to be feasible to use instead of food, like frozen lean tuna (Llave et al. 2016). Llave et al. (2020) simulated the power absorption of two-component materials water and oil; oil represents the frozen materials.

The objectives of this study were:

1. to obtain a finite element model of microwave and microwave infrared combination tempering of frozen potato puree.
2. to obtain electrical field distribution by Maxwell equations to calculate microwave power. In a previous study (Seyhun et al. 2009), the model was obtained by

the finite difference method using Lambert equations to estimate the microwave heating.

3. to analyze the effects of microwave and infrared power on the rate of heat transfer of frozen potato puree, separately and the change of temperature in relation to the position in the frozen potato puree.
4. to validate the model by the experimental data.

Mathematical Model Development

Assumptions

- The effect of evaporation on heat transfer was not considered. Similarly, since the moisture loss during microwave melting was about 1% or less, the evaporation corresponding to this small amount of moisture loss was neglected in the heat transfer during tempering (Chamchong and Datta 1999).
- In the impedance boundary condition, resistive metal losses were expected to be small.

Microwave Heating Mathematical Formulation

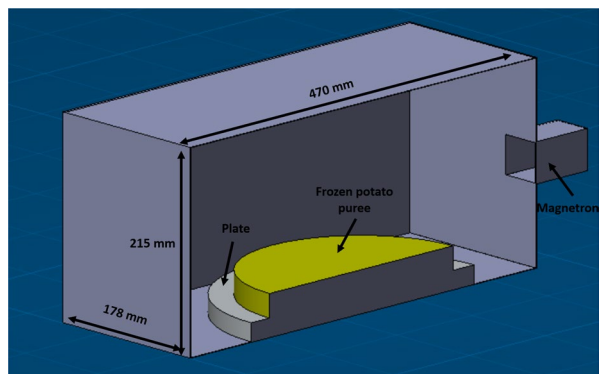
In the model, frozen potato was placed on top of a porcelain plate and placed at the center of the oven. The physical geometry of the rectangular waveguide, the entire oven, and potato was sketched in Fig. 1.

With the assumptions, the non-linear heat transfer equation of a cylindrical slab was expressed as:

$$\frac{\partial(C_p \rho T)}{\partial t} = \nabla(k \nabla T) + Q_{\text{gen}} \quad (1)$$

where Q_{gen} is the volumetric heat generation term (W/m^3), C_p is the specific heat capacity ($\text{J}/\text{kg}^\circ\text{C}$), ρ is the density (kg/m^3), T is the temperature ($^\circ\text{C}$), t is the time

Fig. 1 Sketch used for modeling of the entire oven together with rectangular waveguide and potato



(s), and k is the thermal conductivity (W/m°C). During thawing, the density of food was assumed constant as similarly done in earlier studies (Lucas et al. 2000; Cham-chong and Datta 1999).

To solve the non-linear heat transfer equation, the initial and boundary conditions were used as below. On the symmetry line, no heat transfer takes place, so the heat flux was equal to zero. It was assumed that heat transfer on the surface of the food was by convection.

$$@t = 0, T = T_0 \quad (2)$$

$$@z = 0, n \cdot (k\nabla T) = h_T(T_{\text{inf}} - T) \quad (3)$$

$$@z = L, n \cdot (k\nabla T) = 0 \quad (4)$$

T_{inf} is the air temperature in the oven (°C), T_0 is the initial temperature (°C), h_T is the heat transfer coefficient (W/(m²·°C)), and n is a unit vector that is normal to the surface.

Electric Field Determination by Maxwell Equations

Volumetric heat generation should be obtained to solve the heat transfer equation. Microwave energy absorbed by the food per unit time can be determined by the Poynting theorem:

$$Q_{\text{gen}}(x, y, z, t) = 2\pi f \epsilon_0 \epsilon'' |E|^2 \quad (5)$$

where E is the electric field (V/m), f is the frequency, ϵ'' is the dielectric loss factor, and ϵ_0 is the dielectric constant of free space (8.854×10^{-12} F/m).

During tempering of potato, the power absorbed and electric field distribution inside the oven were obtained by solving the Maxwell's equation for time changing dielectric property. James Clerk Maxwell in 1873 described electromagnetic heating of microwave as a set of four basic equations.

$$\nabla \times E = -j\omega\mu H \quad \text{Faraday's Law} \quad (6)$$

$$\nabla \times H = J + j\omega\epsilon E \quad \text{Ampere's Law} \quad (7)$$

$$\nabla \cdot \epsilon E = \rho \quad \text{Gauss's Laws} \quad (8)$$

$$\nabla \cdot \mu H = 0 \quad \text{Gauss's magnetic law} \quad (9)$$

where ϵ is the permittivity (F/m), μ is the permeability (H/m), H is the magnetic field intensity (A/m), ρ is the density of charge (kg/m³), ω is the angular frequency (rad/s), J is the current flux (A/m²), and $j = \sqrt{-1}$.

Transverse electric (TE) wave was used to excite the rectangular waveguide of the oven. TE₁₀ propagation mode was selected since the microwave oven frequency was

2.45 GHz. Malafronte et al. (2012) obtained the electric field equation as electromagnetic energy was transferred through a rectangular waveguide with TE₁₀ wave propagation mode.

$$\nabla \times \mu_r^{-1}(\nabla \times E) - k_0^2 \left(\epsilon_r - \frac{j\sigma}{\omega\epsilon_0} \right) E = 0 \quad (10)$$

where μ_r is the sample relative permeability equal to 1, ω is the angular frequency (rad/s), σ is the sample electric conductivity (S/m), and ϵ_r is the sample relative permittivity equal to 1.

Initial, boundary, and excitation conditions for electric field determination by Maxwell equations are given in Table 1.

Infrared Heating Mathematical Formulation

The infrared heating can be calculated by the Stefan-Boltzmann Law.

$$Q = \epsilon \sigma (T_s^4 - T^4) \quad (17)$$

where T_s is the halogen lamp surface temperature (K), ϵ is the surface emissivity, T is the food temperature (K), and σ is the Stefan-Boltzmann constant (5.67×10^{-8} W/m²·K⁴).

Model and Experimental Input

Temperature

The experimental temperature data at 0.5 cm, 1.5 cm, and 2.5 cm deep from the surface of potato tempered in the same oven that was modeled was obtained from the study of Seyhun et al. (2009).

Thermal Conductivity

The equation obtained by Choi and Okos (1986) was used for the thermal conductivity of frozen potato:

$$k(T) = 2.01 + 1.39 \times 10^{-3} \times T - 4.33 \times 10^{-6} \times T^2 \quad (18)$$

where T is the temperature (°C) and k is the thermal conductivity (W/m°C).

Specific Heat Capacity

The equation obtained from Seyhun et al. (2009) was used for the specific heat capacity of frozen potato:

Table 1 Initial, boundary, and excitation conditions for electric field determination by Maxwell equations

Equation number	Equation	Explanation
11	$t=0, E_x = E_y = E_z = 0$	At time equals 0, the electric field in the oven was zero in all directions.
12	$E_{in}(z) = E_0 \cos\left(\frac{z\pi}{a}\right)$	By the port, the electromagnetic field was excited in z direction with Eq. 12 (Curet et al. 2014).
13	$n \times E = 0$	The walls of the oven were assumed to be perfect conductors and the tangential electric field component was set to be zero in the equation.
14	$n \times H = 0$	At the symmetry line, magnetic field was zero.
15	$\beta = \frac{2\pi}{c} \sqrt{v^2 - v_c^2}$	The propagation constant β was determined from the equation, where v_c is the cut-off frequency and c is the speed of light.
16	$(v_c)_{mn} = \frac{c}{2} \sqrt{\left(\frac{m}{a}\right)^2 + \left(\frac{n}{b}\right)^2}$	The cut-off frequency can be calculated by Eq. 16 (Singh and Verma 2009).

$$C_p(T) = 2087.8 + 21.058 \times T + 0.2224 \times T^2 \quad (19)$$

where C_p is the specific heat capacity (J/kg°C) and T is the temperature (°C).

Dielectric Properties

In some studies, the dielectric properties of food varied slightly with temperature and moisture content (Yazicioglu et al. 2021); thus, they were assumed constant in the simulation. However, the dielectric constant and the dielectric loss factor of frozen potato during thawing were significantly changing as temperature changes (Seyhun et al. 2009). Data presented in the study was used and dielectric constant (ϵ') and dielectric loss factor (ϵ'') change in relation to temperature was fitted to the equations listed below using Microsoft Excel software package (Microsoft Corporation, USA) with R^2 values 0.9932 and 0.9969, respectively.

$$\epsilon'(T) = 0.0029T^3 + 0.2104T^2 + 5.0149T + 43.256 \quad (20)$$

$$\epsilon''(T) = 0.0009T^3 + 0.0661T^2 + 1.6036T + 13.424 \quad (21)$$

The complex forms of dielectric properties were used for calculation of microwave power by Maxwell equations $\epsilon'(T) - \epsilon''(T)j$.

Modeling

Maxwell equations were calculated for the entire oven by the finite element method using Comsol Multiphysics software v.4.3 (Comsol Inc., Burlington, MA, USA). To ease the calculation, the oven was divided into two symmetrical parts. The oven (Advantium oven, General Electric Company, Louisville, KY, USA) was drawn as a rectangular box according to the dimensions given in the user manual. Potato was placed at the midpoint on the porcelain plate that was drawn as a cylindrical slab. Air was defined as no heat transfer medium in the systems. Port boundary was defined on the right surface of the rectangular waveguide. Oven and rectangular waveguide walls were stainless steel; thus, metal boundaries were applied. Parameters and properties of structural steel, air, and porcelain were obtained from the library of the Comsol Multiphysics and listed in Table 2.

Figure 2 shows the flowchart for modeling strategy in the COMSOL software. The model variables and input parameters were defined in variable, functions, and parameter module of the software under Global Definition, respectively. The geometry of the oven was built based on the specified dimensions. For electromagnetic heating, the radio frequency module/microwave heating interface was used. Electric field (E) and temperature (T) were dependent variables of microwave heating interface. The time-dependent solver MUMPS (Multifrontal Massively Parallel sparse direct Solver) and backward differentiation formulas (BDF) were used for time stepping in order to solve Maxwell equations. Initial and boundary conditions were entered in the software. The boundary condition for surface to ambient radiation was used to reflect

Table 2 Parameters used for the simulation

Description	Expression	Source
Width, depth, and height of the oven	$470 \text{ [mm]} \times 356 \text{ [mm]} \times 215 \text{ [mm]}$	Current study
Width, depth, and height of the waveguide	$(86.36/2) \text{ [mm]} \times 70 \text{ [mm]} \times 43.13 \text{ [mm]}$	Current study
Radius and height of the glass plate	$150 \text{ [mm]} \times 20 \text{ [mm]}$	Current study
Base of the glass plate	15 [mm]	Current study
Radius and height of the frozen potato puree	$125 \text{ [mm]} \times 25 \text{ [mm]}$	Current study
Initial temperature of the frozen potato puree	-25 [°C]	Current study
Density of the potato	1395 [kg/m ³]	Seyhun et al. 2009
Heat transfer coefficient for microwave heating	20 [W/(m ² K)]	Seyhun et al. 2009
Heat transfer coefficient for microwave infrared combination heating	30 [W/(m ² K)]	Seyhun et al. 2009
Air temperature in the oven	20 [°C]	Current study
Surface emissivity of frozen potato puree	0.88	Almeida 2005
Surface temperature of the halogen lamp	500 [K]	Current study
Relative permeability and permittivity of air	1	Comsol Multiphysics library
Electrical conductivity of air [S/m]	0	Comsol Multiphysics library
Relative permeability of silicon carbide (porcelain)	1	Comsol Multiphysics library
Relative permittivity of silicon carbide (porcelain)	10	Comsol Multiphysics library
Electrical conductivity of silicon carbide (porcelain) [S/m]	10 ³	Comsol Multiphysics library
Relative permeability and permittivity of structural steel	1	Comsol Multiphysics library
Electrical conductivity of structural steel [S/m]	4.02×10^6	Comsol Multiphysics library

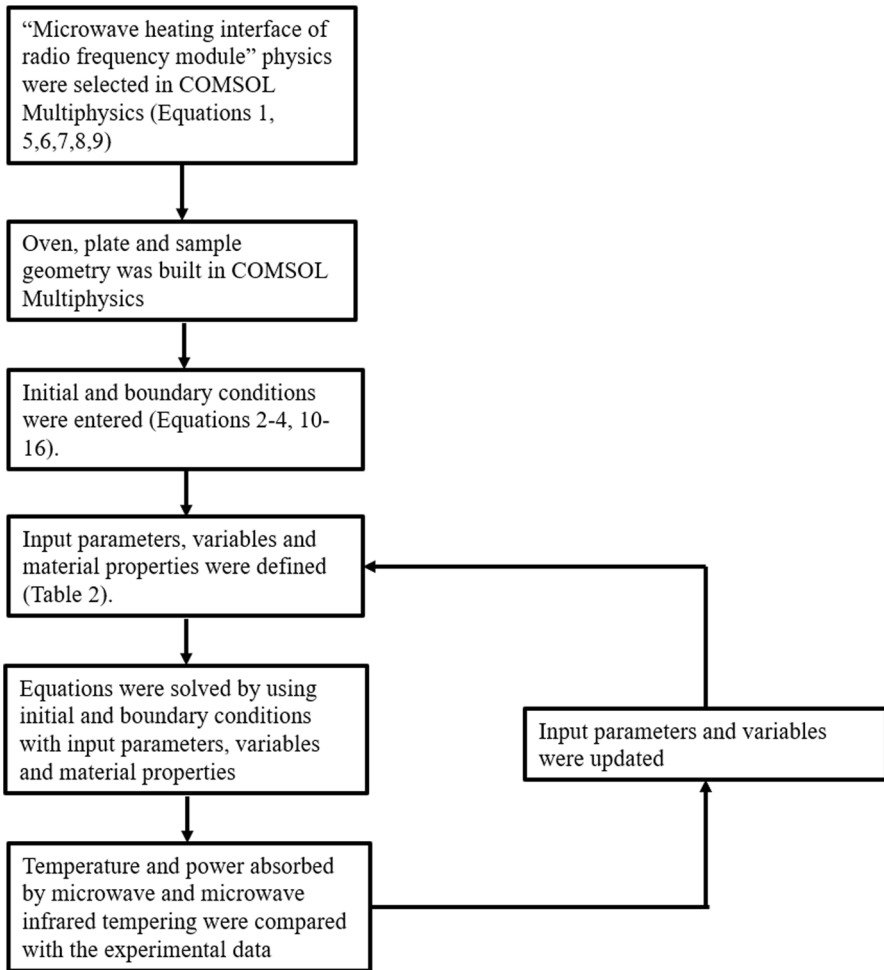


Fig. 2 Flowchart for modeling development in COMSOL software

the surface heating of food by infrared (Eq. 17). Convective heat transfer was modeled using the boundary condition of heat flux at the surface of the food using Eq. 3.

The time required to solve equations with boundary conditions to determine electric field and temperature distributions was 7–9 min by Intel Core™ 2.40 GHz, 16-GB computer. The microwave and infrared energy in the oven was supplied with on and off cycles. Cycles of power have been studied by several researchers (Cham-chong and Datta 1999; Campañone et al. 2012). In this study, a piecewise analytic equation was obtained to reflect the on-off time to the model.

Since the potato was the center of attention, its mesh dimension was chosen to be finer than the rest of the oven parts. Calculated mesh properties are shown in Table 3. Different meshing combinations for different parts of the system were implemented until the simulation results were independent of meshing.

Statistical Analysis

The statistical comparison of the model with the experimental data was obtained by root mean square error (RMSE) using Eq. 22 and Microsoft Excel software package (Microsoft Corporation, USA).

$$\text{RMSE} = \sqrt{\frac{1}{N} \sum_{i=1}^N (T_{\text{model}} - T_{\text{exp}})^2} \quad (22)$$

Results and Discussion

Simulation Results for Microwave Tempering and Comparison with Experimental Results

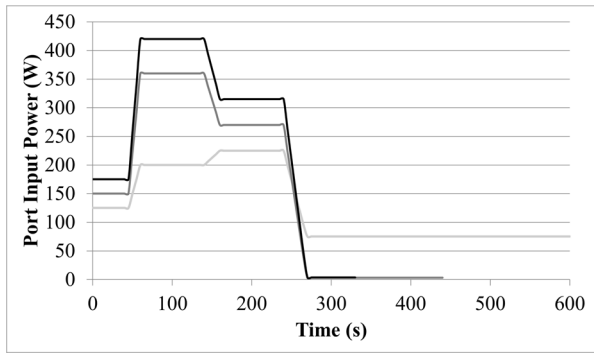
The electromagnetic properties of foods change with temperature significantly below their freezing point (Tanaka et al. 1999). The physical properties of foods change dramatically during thawing with temperature change which has great effect on dielectric constant, dielectric loss factor, and thermal conductivity. According to Sahin and Sumnu (2006), the rate of change of the dielectric constant and the loss factor with respect to temperature depends on the ratio of bound to free moisture content. Since water is in the bound form initially during tempering, the dielectric properties increase dramatically with the temperature increase as melting occurs. The effects of moisture and ash content on dielectric properties of ham at temperatures -35 to 70 °C were studied and found that until melting started at -20 °C to -10 °C, ham possessed low dielectric properties. After melting occurs, the loss factor of ham increases with ash content (Sipahioglu et al. 2003).

The temperature dependence of thermal and electromagnetic properties of frozen potato challenged the modeling study. Thermal conductivity (Eq. 18), specific heat (Eq. 19), dielectric constant (Eq. 20), and dielectric loss factor (Eq. 21) were

Table 3 Mesh properties

Name	Value
Maximum element size	0.041
Minimum element size	0.005
Resolution of curvature	0.5
Resolution of narrow regions	0.6
Maximum element growth rate	1.45
Minimum element quality	0.150
Average element quality	0.728
Tetrahedral elements	5412
Triangular elements	1416
Edge elements	208
Vertex elements	28

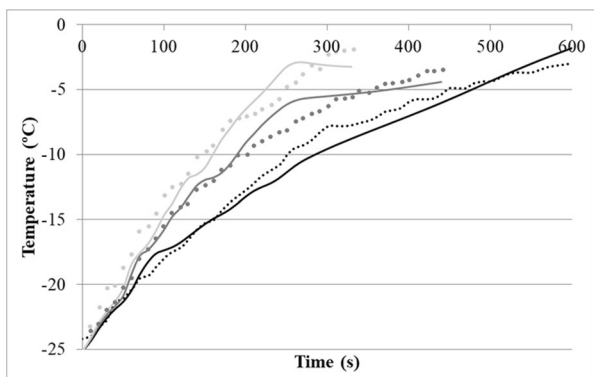
Fig. 3 Port input power for 50% (black), 40% (dark grey), and 30% (light grey) microwave power



introduced to the model in Comsol Multiphysics as a function of temperature, which leads to a rapid increase in the solution time.

In this work, the model and experimental data were fitted by obtaining port input power for microwave power levels. Port input power is shown in Fig. 3. For all microwave power selections, microwave transmission was found to be active up to about 300 s of tempering. Klinbun and Rattanadecho (2021) studied the effect of port position on heating patterns and rates in domestic microwave oven. Port position in this study was drawn and modeled according to the oven. The transient surface (0.5-cm depth) temperature profiles from frozen state until tempering state completed are shown in Fig. 4 for 30%, 40%, and 50% microwave power levels. Tempering state was completed when the surface temperature of the food reached from -5 to -2 °C. The mathematical models were obtained until the experimental tempering was completed in 330 s, 440 s, and 600 s for 50%, 40%, and 30% microwave power, respectively. The comparison between the microwave powers of 30, 40, and 50% was done. As expected, greater power dissipation occurs as microwave power increases. The surface temperature of the frozen potato was linearly increased as microwave power increased. The models showed that the tempering time was reduced 82% when 50% microwave power was selected instead of 30%. Moreover, in the 200-s heating period, the coldest temperature observed was -19 °C for 30% microwave power as it was -13 °C for

Fig. 4 Model (line) and experimental (dotted line) results of surface (0.5-cm depth) temperature of the potato tempered by 30% (grey), 40% (dark grey), and 50% (black) microwave power



50% microwave power (Fig. 5). This can be mainly due to the difference in determined port input power and rapid increase in the dielectric properties of potato as temperature increases. The uneven heating demonstrated by the model (Fig. 5) was because of the mixture of ice and water in the food leading to very different dielectric properties. Since the dielectric loss factor of ice is lower than that of water, ice absorbs less energy, causing a partial melting of the ice and runaway heating. One part of the food may cook whilst the other parts may be still frozen. This may be prevented by application of pulse microwave energy and allowing the temperature to come to equilibrium in the interval (Smith 2011).

The simulated temperature profiles at three internal locations were compared with the experimental counterpart for tempering at 30%, 40%, and 50% microwave power levels, respectively (Fig. 6). The root mean square error (RMSE) values are given in Table 4. Temperature models were in good agreement with the experimental data with root mean square error (RMSE) ranging from 0.55 to 1.16 °C with an average of 0.76 °C. This result proves that the estimation of port input power during tempering was accurate.

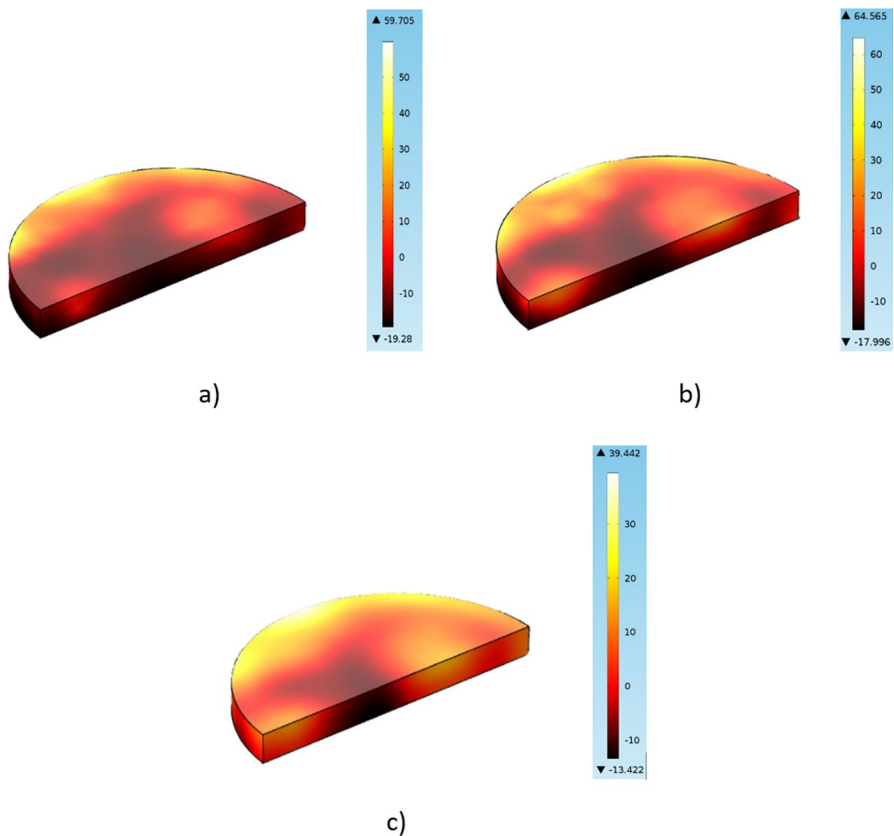


Fig. 5 Simulated temperature profile of potato puree after 200 s of tempering by **a** 30%, **b** 40%, and **c** 50% microwave power

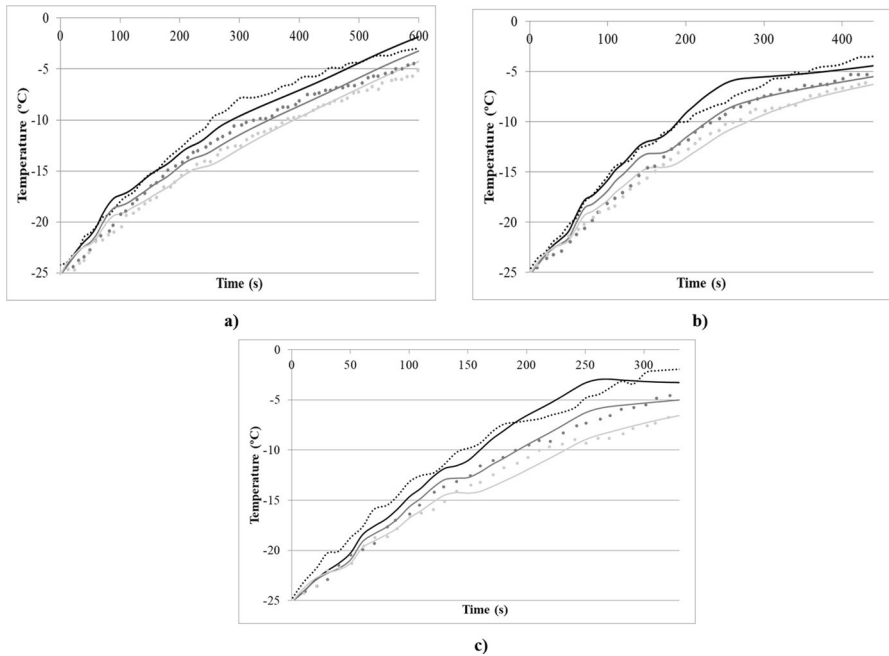


Fig. 6 Model (line) and experimental (dotted line) results of temperature at 0.5 cm (black), 1.5 cm (dark grey), and 2.5 cm (grey) depth of the potato tempered by **a** 30%, **b** 40%, and **c** 50% microwave power

Table 4 Root mean square errors (RMSE) calculated by experimental data and simulation models obtained for temperature (°C) at different depths of potato

Microwave power (%)	Infrared power (%)	0.5 cm	1.5 cm	2.5 cm
30	0	0.83	0.74	0.65
40	0	0.77	0.84	0.63
50	0	1.16	0.55	0.67
30	10	0.91	0.80	0.76
40	10	0.98	0.84	1.22
50	10	0.89	1.22	0.54

Miran and Palazoğlu (2019) developed a numerical model for microwave tempering of shrimp for two different power levels (500 W and 1 kW) and obtained RMSE values for different positions such as for center 3.9 °C and mid 4.1 °C. Altin et al. (2022) used radio frequency processing for tempering and thawing, developed comprehensive mathematical model and validated the model by experimental data from frozen tuna samples with RMSE values ranging from 0.16 to 0.7°C.

In addition, the variation of temperature with respect to position (0.5 cm, 1.5 cm, and 2.5 cm deep from the surface) in the potato specimen was simulated by the model obtained by Maxwell equations (Fig. 6). The highest temperature

observed was on the surface of the potato, then comes center and bottom temperature, respectively. Curet et al. (2008) studied the numerical and experimental heating by microwave process in frozen and defrosted zones of tylose. Experimental temperature data of the probe placed near the surface was found to be higher than the inside temperature probe data which was consistent with the Maxwell model results. They found that in the frozen zone, Lambert's Law estimation gave less accurate results with respect to Maxwell's equations. They concluded that for low dielectric materials like frozen foods, the electric field calculation was essential in order to predict the temperature distribution effectively into the product since the frozen phase temperature change was very dependent on dielectric properties. Farag et al. (2008) compared radio frequency (RF) tempering of beef meat blends by conventional methods and found that the surface temperature of the meat tempered by RF was higher than the inside temperature.

The deviation of the Maxwell model (Fig. 6) from the experimental data occurred mainly in the tempering region, when temperature ranges from $-5\text{ }^{\circ}\text{C}$ to $-2\text{ }^{\circ}\text{C}$. The reason for this deviation is that in the transition region the thermal and physical properties of the food change significantly (Cevoli et al. 2018; Muthukumarappan et al. 2019) because frozen and non-frozen regions are present simultaneously.

Simulation Results for Microwave-Infrared Combination Tempering and Comparison with Experimental Results

As can be seen from the first part of the study, the microwave simulation performance was good in predicting the experimental literature data. In this part of the study, addition of infrared energy emitted from a halogen lamp was simulated by the boundary condition of surface to ambient radiation using Eq. (17). The on-off cycle of the infrared energy was more dominant than the microwave cycles, since dielectric properties were low during the frozen period. Infrared energy was found to be 7 s on and 38 s off when 10% infrared power was selected in the oven and modeled as a piecewise equation for infrared.

The simulated temperature profiles at three internal locations were compared with the experimental counterpart for tempering at 30%, 40%, and 50% microwave and 10% infrared power combinations, respectively (Fig. 7). Simulated temperatures for microwave-infrared combination were in good agreement with the experimental data with RMSE ranging from 0.54 to 1.22 $^{\circ}\text{C}$ with an average of 0.90 $^{\circ}\text{C}$ (Table 4). This result proves that the estimation of on-off cycle times was accurate. The numerical models were obtained until the experimental tempering was completed in 320 s, 240 s, and 210 s, for 30%, 40%, and 50% microwave and 10% infrared power combinations, respectively. Surface heating was rapid in near-infrared radiation energy which was supplied by halogen lamp since it provides higher frequency and lower penetration depth than the other infrared generators. This case was demonstrated by the highest temperature on the surface (0.5-cm depth) compared with the center and bottom temperatures (Fig. 7).

Figure 8 shows results of surface (0.5-cm depth) temperature of the potato tempered by 30% microwave power and 30% microwave and 10% infrared

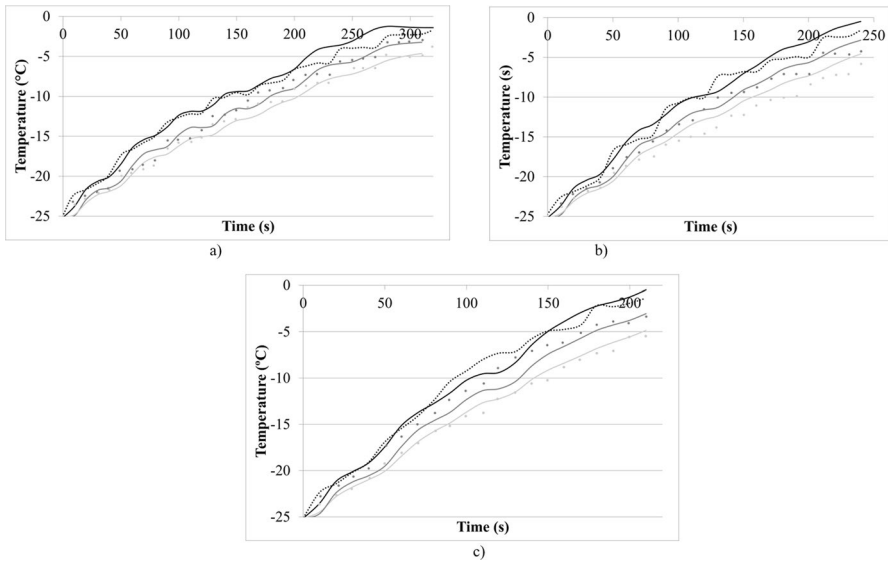
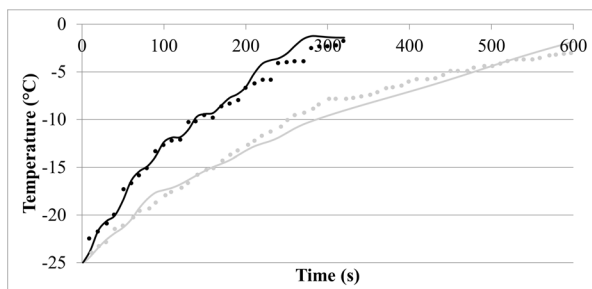


Fig. 7 Model (line) and experimental (dotted line) results of temperature at 0.5 cm (black), 1.5 cm (dark grey), and 2.5 cm (grey) depth of the potato tempered by **a** 30%, **b** 40%, and **c** 50% microwave power and 10% infrared power combinations

power combinations. It shows how addition of infrared energy affected the system. The tempering time was reduced to 320 s by addition of 10% infrared power to 30% microwave power which achieves tempering in 600 s. There is a rapid increase in the surface temperature up to $-6.7\text{ }^{\circ}\text{C}$ for 30% microwave and 10% infrared power whilst it was around $-12.6\text{ }^{\circ}\text{C}$ for 30% microwave power in 200 s of tempering.

The reason why Figs. 7 and 8 do not exactly match the model data may be found in the assumptions made during simulation. The sources of error could be the assumptions of uniform initial temperature distribution and convective heat transfer coefficient throughout the product, and neglecting the mass transfer in the product during thawing tempering region (Klinbun and Rattanadecho 2019; Chen et al. 2016).

Fig. 8 Model (line) and experimental (dotted line) results of surface (0.5-cm depth) temperature of the potato tempered by 30% microwave power (grey) and 30% microwave and 10% infrared power (black)



Conclusion

Modeling heat transfer of frozen potato during tempering in microwave-infrared combination oven was challenging since the thermal and dielectric properties were significantly changing by temperature change. Maxwell equations were used for calculation of microwave power. Port input power for microwave heating was simulated by time. In total, 18 different simulations were run corresponding to 30%, 40%, and 50% microwave and 30% microwave-10% infrared, 40% microwave-10% infrared, and 50% microwave-10% infrared combinations for each of different positions of potato (0.5 cm, 1.5 cm, and 2.5 cm deep from the surface). Models were in good agreement with the experimental data. Average RMSE values were 0.76 °C for microwave and 0.90 °C for microwave and infrared combinations. This study also shows addition of infrared energy decreased the microwave tempering time by 46.6%. Moreover, microwave and infrared powers' effects on rate of tempering were determined. In this study, the viability of simulating the dielectric heating combined with infrared heating of a real frozen food, potato puree, was evaluated and confirmed by experimental data. These results would provide helpful information for designing industrial-scale microwave infrared tempering systems.

Author Contribution Nalan Yazicioglu: conceptualization, methodology, modeling, investigation, writing, reviewing, and editing.

Declarations

Conflict of Interest The author declares no competing interests.

References

- Almeida MF (2005) Modeling infrared and combination infrared-microwave heating of foods in an oven. PhD Dissertation, Cornell University, Ithaca, NY
- Altin O, Marra F, Erdogdu F (2022) Computational study for natural convection effects on temperature during batch and continuous industrial scale radio frequency tempering/thawing processes. *J Food Eng* 312:110743
- Basak T (2003) Analysis of resonances during microwave thawing of slabs. *Int J Heat Mass Transf* 46(22):4279–4301
- Calay R, Newborough M, Probert D, Calay P (1994) Predictive equations for the dielectric properties of foods. *Int J Food Sci Technol* 29(6):699–713
- Campañone LA, Zaritzky NE (2010) Mathematical modeling and simulation of microwave thawing of large solid foods under different operating conditions. *Food Bioprocess Technol* 3(6):813–825
- Campañone LA, Paola CA, Mascheroni RH (2012) Modeling and simulation of microwave heating of foods under different process schedules. *Food Bioprocess Technol* 5(2):738–749
- Cevoli C, Fabbri A, Tylewicz U, Rocculi P (2018) Finite element model to study the thawing of packed frozen vegetables as influenced by working environment temperature. *Biosyst Eng* 170:1–11
- Chamchong M, Datta AK (1999) Thawing of foods in a microwave oven: I. Effect of power levels and power cycling. *J Microw Power Electromagn Energy* 34(1):9–21
- Chen J, Pitchai K, Birla S, Jones D, Negahban M, Subbiah J (2016) Modeling heat and mass transport during microwave heating of frozen food rotating on a turntable. *Food Bioprod Process* 99:16–127
- Choi Y, Okos MR (1986) Effects of temperature and composition on the thermal properties of food. In: Le Maguer M, Jelen P (eds) *Food engineering and process applications, transport phenomena*, vol 1. Elsevier Applied Science Publishers, London, pp 93–101

- Curet S, Rouaud O, Boillereaux L (2008) Microwave tempering and heating in a single-mode cavity: numerical and experimental investigations. *Chem Eng Process Process Intensif* 47(9-10):1656–1665
- Curet S, Rouaud O, Boillereaux L (2014) Estimation of dielectric properties of food materials during microwave tempering and heating. *Food Bioprocess Technol* 7(2):371–384
- Dincov DD, Parrott KA, Pericleous KA (2004) Heat and mass transfer in two-phase porous materials under intensive microwave heating. *J Food Eng* 65(3):403–412
- Erdogdu F, Karatas O, Sarghini F (2018) A short update on heat transfer modelling for computational food processing in conventional and innovative processing. *Curr Opin Food Sci* 23:113–119. ISSN 2214-7993. <https://doi.org/10.1016/j.cofs.2018.10.003>
- Farag KW, Lyng JG, Morgan DJ, Cronin DA (2008) A comparison of conventional and radio frequency tempering of beef meats: effects on product temperature distribution. *Meat Sci* 80(2):488–495
- James SJ, James C, Purnell G (2017) 12 - Microwave-assisted thawing and tempering. In: Marc R, Kai K, Helmar S (ed) *The microwave processing of foods* (2nd edn). Woodhead Publishing Series in Food Science, Technology and Nutrition, Woodhead Publishing, Sawston, UK, pp 252–272. <https://doi.org/10.1016/B978-0-08-100528-6.00012-7>
- Klinbun W, Rattanadecho P (2017) An investigation of the dielectric and thermal properties of frozen foods over a temperature from –18 to 80°C. *Int J Food Prop* 20(2):455–464. <https://doi.org/10.1080/10942912.2016.1166129>
- Klinbun W, Rattanadecho P (2019) Effects of power input and food aspect ratio on microwave thawing process of frozen food in commercial oven. *J Microw Power Electromagn Energy* 53(4):225–242
- Klinbun W, Rattanadecho P (2021) Numerical study of initially frozen rice congee with thin film resonators package in microwave domestic oven. *J Food Process Eng* e13924
- Llave Y, Mori K, Kambayashi D, Fukuoka M, Sakai N (2016) Dielectric properties and model food application of tylose water pastes during microwave thawing and heating *J Food Eng* 178:20–30 ISSN 0260-8774. <https://doi.org/10.1016/j.jfoodeng.2016.01.003>
- Llave Y, Kambayashi D, Fukuoka M, Sakai N (2020) Power absorption analysis of two-component materials during microwave thawing and heating: Experimental and computer simulation. *Innovative Food Sci Emerg Technol* 66:102479
- Lucas T, Flick D, Chourot JM, Raoult-Wack AL (2000) Modeling and control of thawing phenomena in solute-impregnated frozen foods. *J Food Eng* 45(4):209–218
- Malafrente L, Lamberti G, Barba AA, Raaholt B, Holtz E, Ahrné L (2012) Combined convective and microwave assisted drying: experiments and modeling. *J Food Eng* 112:304–312
- Miran WT, Palazoğlu K (2019) Development and experimental validation of a multiphysics model for 915 MHz microwave tempering of frozen food rotating on a turntable. *Biosyst Eng* 180:191–203. <https://doi.org/10.1016/j.biosystemseng>
- Muthukumarappan K, Marella C, Sunkesula V (2019) Food freezing technology. In: *Handbook of farm, dairy and food machinery engineering*. Academic Press, Cambridge, Massachusetts, pp 389–415
- Pitchai K, Chen J, Birla S, Jones D, Gonzalez R, Subbiah J (2015) Multiphysics modeling of microwave heating of a frozen heterogeneous meal rotating on a turntable. *J Food Sci* 80:2803–2814. <https://doi.org/10.1111/1750-3841.13136>
- Ramaswamy H, Tang J (2008) Microwave and radio frequency heating. *Food Sci Technol Int* 14(5):423–427
- Rattanadecho P, Aoki K, Akahori M (2002) A numerical and experimental investigation of the modelling of microwave heating for liquid layers using a rectangular wave guide (effects of natural convection and dielectric properties). *Appl Math Model* 26(3):449–472
- Sahin S, Sumnu SG (2006) Electromagnetic properties. In: Heldman DR (ed) *Physical properties of foods*. Springer Science & Business Media, New York, pp 167–171
- Sepúlveda GV, Barbosa-Cánovas (2003) Heat transfer in food products. In: Welti-Chanes J, Véllez-Ruiz JF, Barbosa-Cánovas GV (eds) *Transport phenomena in food processing*, CRC Press, Boca Raton, FL
- Seyhun N, Ramaswamy H, Sumnu G, Sahin S, Ahmed J (2009) Comparison and modeling of microwave tempering and infrared assisted microwave tempering of frozen potato puree. *J Food Eng* 92(3):339–344. ISSN 0260-8774. <https://doi.org/10.1016/j.jfoodeng.2008.12.003>
- Singh A, Verma S (2009) *Fundamentals of microwave engineering: principles, waveguides, microwave amplifiers and applications*. PHI Learning Private Limited, New Delhi
- Singh D, Singh D, Husain S (2020) Computational analysis of temperature distribution in microwave-heated potatoes. *Food Sci Technol Int* 26(6):465–474

- Sipahioglu O, Barringer SA, Taub I (2003) Modelling the dielectric properties of ham as a function of temperature and composition. *J Food Sci* 68:904–908
- Smith P (2011) Mass transfer operations. In: *Introduction to food process engineering*. Springer, Boston, MA, pp 184
- Taher BJ, Farid MM (2001) Cyclic microwave thawing of frozen meat: experimental and theoretical investigation. *Chem Eng Process* 40(4):379–389
- Tanaka F, Mallikarjunan P, Hung YC (1999) Dielectric properties of shrimp related to microwave frequencies: from frozen to cooked stages. *J Food Process Eng* 22(6):455–468
- Vegh V, Turner IW (2006) A hybrid technique for computing the power distribution generated in a lossy medium during microwave heating. *J Comput Appl Math* 197(1):122
- Venugopal V (2005) Quick freezing and individually quick frozen products. In: Venugopal V (ed) *Seafood processing: adding value through quick freezing, retortable packaging and cook-chilling*. CRC Press, Boca Raton, Florida, pp 95–139
- Yazicioglu N, Sumnu G, Sahin S (2021) Heat and mass transfer modeling of microwave infrared cooking of zucchini based on Lambert law. *J Food Process Eng* 44(12):e13895

Publisher's Note Springer Nature remains neutral with regard to jurisdictional claims in published maps and institutional affiliations.

Springer Nature or its licensor (e.g. a society or other partner) holds exclusive rights to this article under a publishing agreement with the author(s) or other rightsholder(s); author self-archiving of the accepted manuscript version of this article is solely governed by the terms of such publishing agreement and applicable law.